PNAS

Supplementary Information for

Title: Lipopolysaccharide-induced sepsis impairs M2R-GIRK signaling in the mouse sinoatrial node

Niroj Shrestha[a,1], Klaus Zorn-Pauly[a,1], Pietro Mesirca[b,c], Chintan N. Koyani[d], Gerald Wölkart[e], Valentina Di Biase[f], Eleonora Torre[b,c], Petra Lang[a], Astrid Gorischek[a], Wolfgang Schreibmayer[a], Robert Arnold[a], Heinrich Maechler[g], Bernd Mayer[e], Dirk von Lewinski[d], Angelo G. Torrente[b,c], Matteo E. Mangoni[b,c], Brigitte Pelzmann[a,2], Susanne Scheruebel[a,2]

[a]Gottfried Schatz Research Center for Cell Signaling, Metabolism and Aging, Medical Physics and Biophysics, Medical University of Graz, 8010 Graz, Austria

[b]Institut de Génomique Fonctionnelle, Université de Montpellier, CNRS, Inserm, 34094 Montpellier, France

[c]Laboratory of Excellence in Ion Channels Science and Therapeutics, 34094 Montpellier, France

[d]Division of Cardiology, Medical University of Graz, 8036 Graz, Austria

[e]Department of Pharmacology and Toxicology, University of Graz, 8010 Graz, Austria

[f]Institute of Pharmacology, Medical University of Innsbruck, 6020 Innsbruck, Austria

[g]Division of Cardiac Surgery, Medical University of Graz, 8036 Graz, Austria

[1]These authors contributed equally to the work.

[2]Correspondance email: brigitte.pelzmann@medunigraz.at

susanne.scheruebel@medunigraz.at

This PDF file includes:

Figures S1 to S7

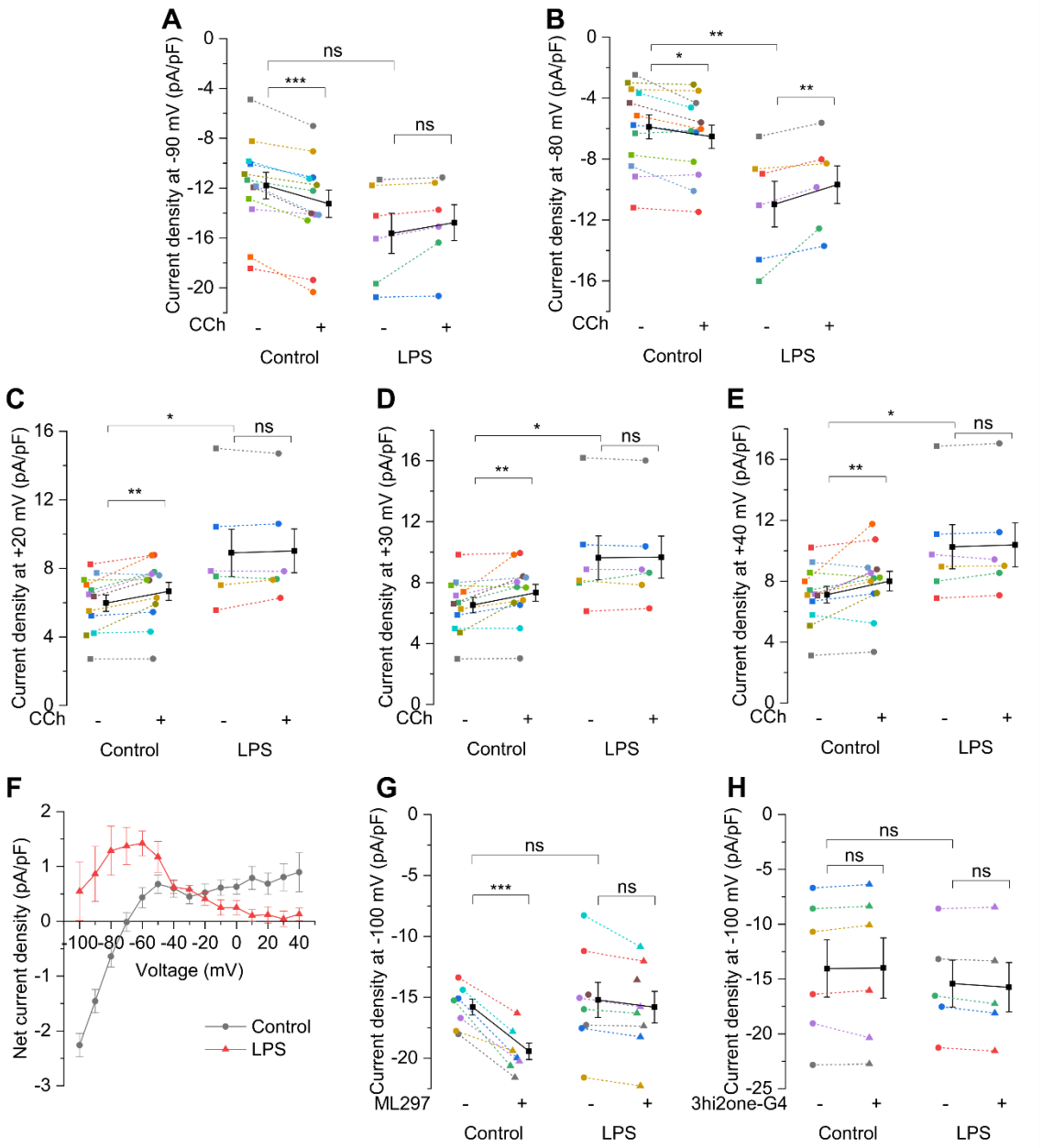

Fig. S1. LPS inhibits CCh- and ML297-mediated increase in steady-state current density in isolated SAN cells. Scatter plots with mean ± SEM for current density at -90, -80, +20, +30 and +40 mV for ramps in Fig. 3A, 3B in the absence (-) and presence (+) of 0.1 µM CCh (A-E) and at -100 mV in the absence (-) and presence (+) of 3 µM ML297 (G) and 30 µM 3hi2one-G4 (H) in the SAN cells isolated from LPS-injected mice. (F) Traces showing mean ± SEM of difference current (I_{CCh}-I_{basal}, CCh-induced) density from -100 to +40 mV ramp over 1.5 s in the SAN cells from control vs. LPS-injected mice. N = 6 (A-F), N = 8 (G)) vs controls (N = 12 (A-F), N = 7 (G); *p < 0.05, **p < 0.01, ***p<0.001, ^{ns}p > 0.05; mixed two-way ANOVA followed by simple effect analysis.

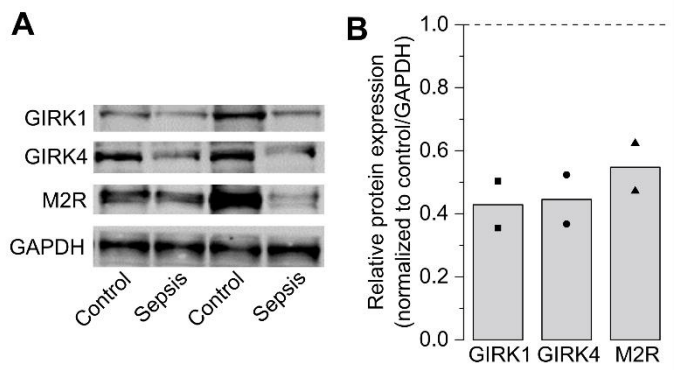

Fig. S2. Reduced expression of M2R and GIRK1/4 channels in human right atrial appendages (RAA) in sepsis. (A) Western blots and (B) densitometric evaluation of immunoreactive bands showing reduced expression of GIRK1, GIRK4 and M2R in RAA of septic patients compared to control patients. GAPDH is used as a loading control. Bars represent mean and symbols represent independent experiments (N = 2).

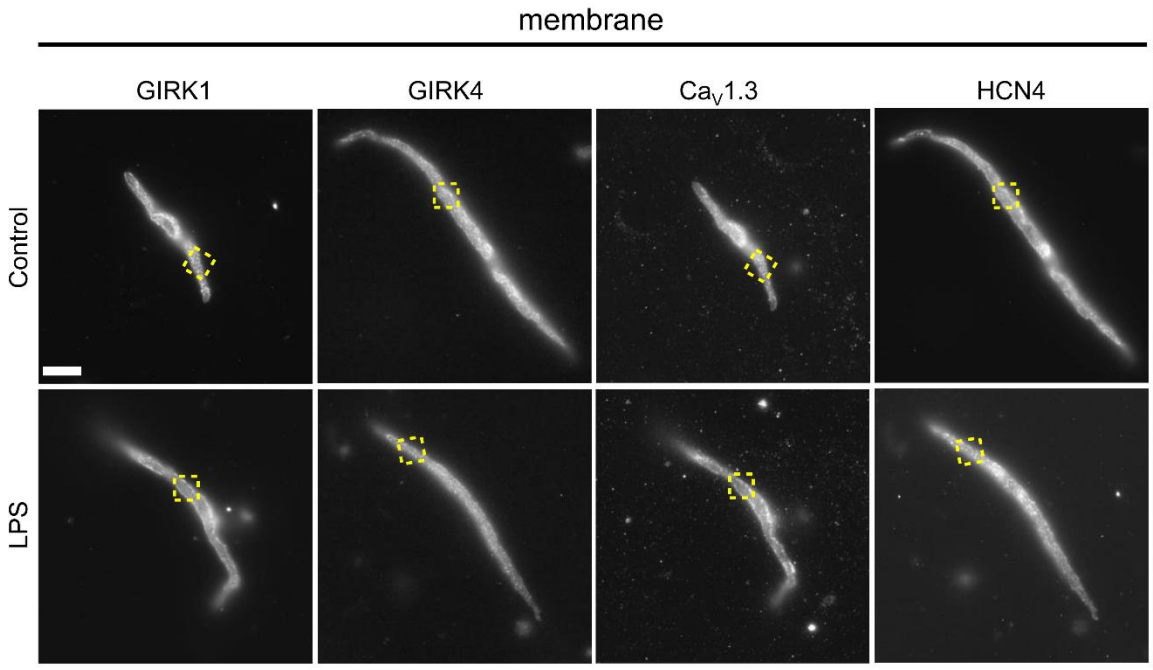

Fig. S3. LPS reduces expression of ion-channels in SAN cells involved in parasympathetic modulation. Representative immunofluorescence images of SAN cells isolated from control (above) and LPS-injected (below) mice showing membrane expression of GIRK1, GIRK4, $Ca_v1.3$ and HCN4. The focal plane is placed at the level of the cell membrane adhering to the coverslip identified by the HCN4 and GIRK1 staining (see Fig. S4 for further information). The magnified membrane sections shown in Fig. 4C were isolated from these cells (yellow dashed squares). Scale bar = 20 µm.

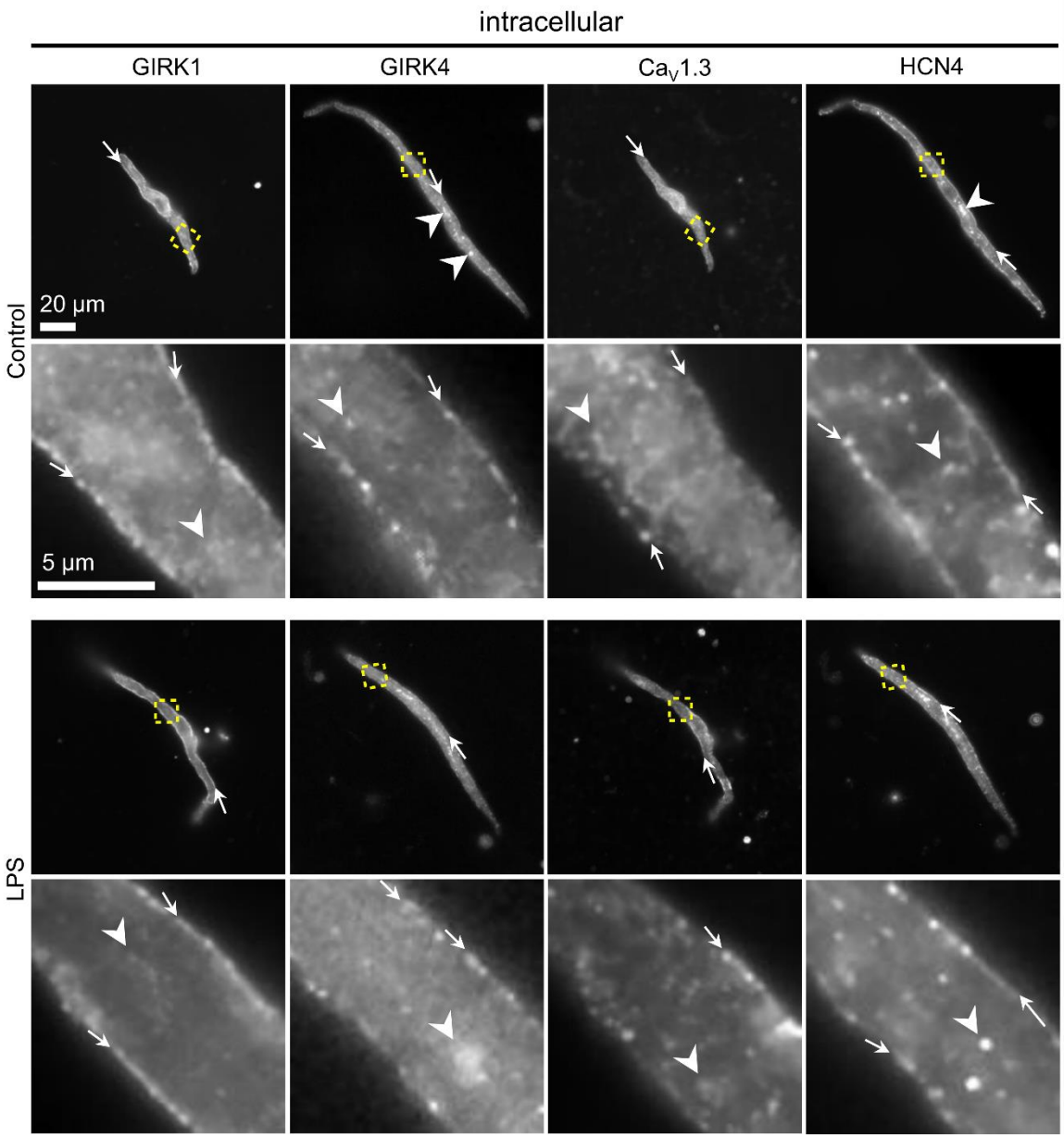

Fig. S4. Representative longitudinal intracellular section of immunolabelled SAN cells from control and LPS-injected mice. The low magnification panels (first and third rows) show the same SAN cells presented in Fig. S3 with the longitudinal focal plane passing through the cells. The anti-GIRK1, GIRK4, $Ca_V1.3$ and HCN4 staining outline marked membrane localization visible as a rim surrounding the cells (arrows). The regions contained in the yellow dashed boxes are enlarged in the below panels (second and fourth rows) and correspond to the membrane regions shown in Fig. 4C. Some intracellular labeling consistent with organelle localization (arrowheads) was segregated in restricted domains well apart from the cell membrane (arrows).

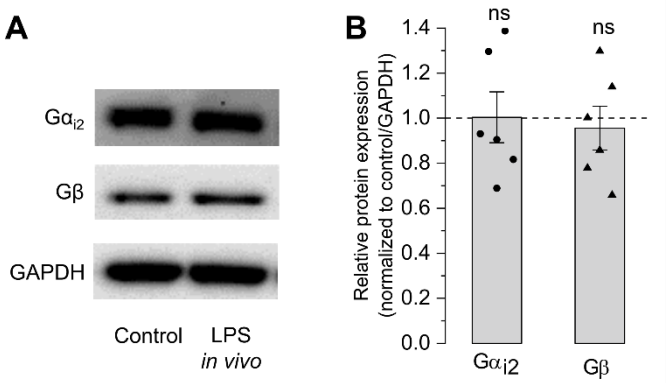

Fig. S5. LPS does not affect expression of G-protein subunits in isolated SAN tissues. (A) Representative western blots and (B) scatter plot of densitometric evaluation of immunoreactive bands showing similar expression of $G\alpha_{i2}$ and Gβ in SAN tissues after 6 h of LPS i.p. injection in mice (*in vivo*). GAPDH is used as a loading control. Data are expressed as symbols (independent experiments, N = 6) with mean ± SEM as bars, $^{ns}p > 0.05$, one-sample t-test.

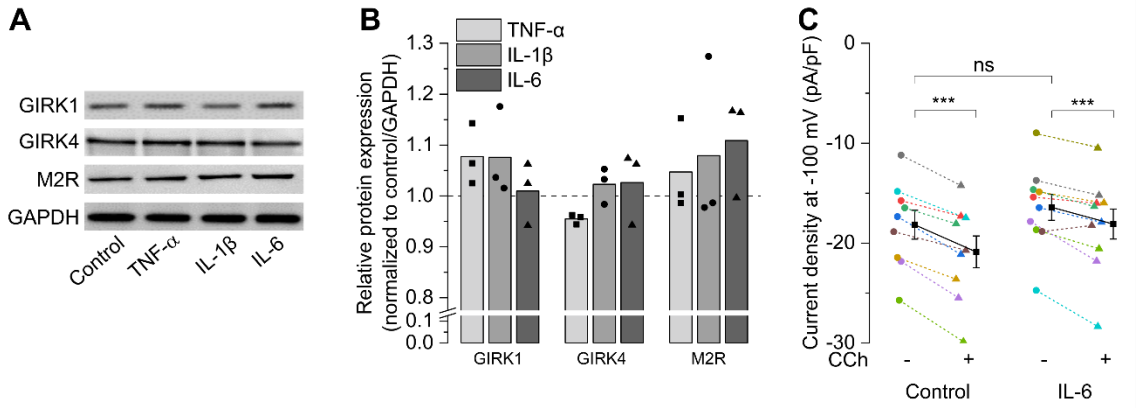

Fig. S6. Pro-inflammatory cytokines do not directly alter expression of M2R and GIRK1/4 channels in isolated SAN tissues. (A) Representative western blots and (B) densitometric evaluation of immunoreactive bands showing absence of reduced expression of GIRK1, GIRK4 and M2R in mouse SAN tissue after 6 h incubation with TNF-α, IL-1β and IL-6. GAPDH is used as a loading control. Bars represent mean and symbols represent independent experiments (N = 3). (C) Scatter plot with mean ± SEM for current density at -100 mV in the absence (-) and presence (+) of 0.1 µM CCh in the isolated control SAN cells preincubated without or with 10 ng/ml IL-6 for 2 h (N = 9, controls; N = 10, IL-6). ***p<0.001, $^{ns}p > 0.05$; mixed two-way ANOVA followed by simple effect analysis.

Fig. 4A

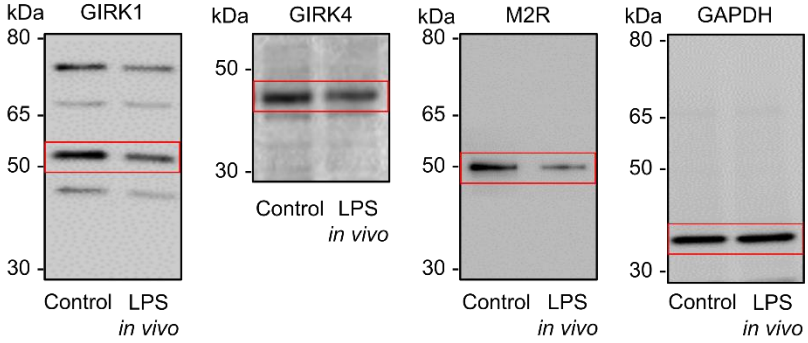

Fig. 4B

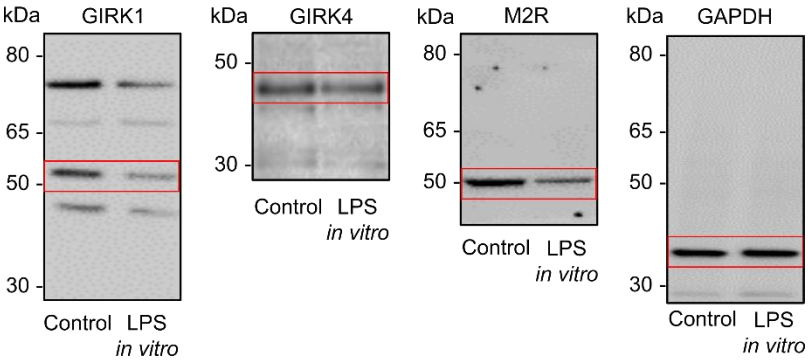

73

Fig. S2A

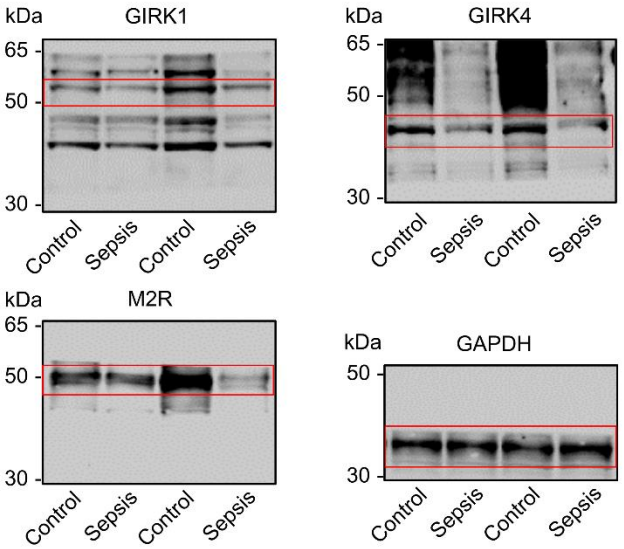

74

Fig. S5A

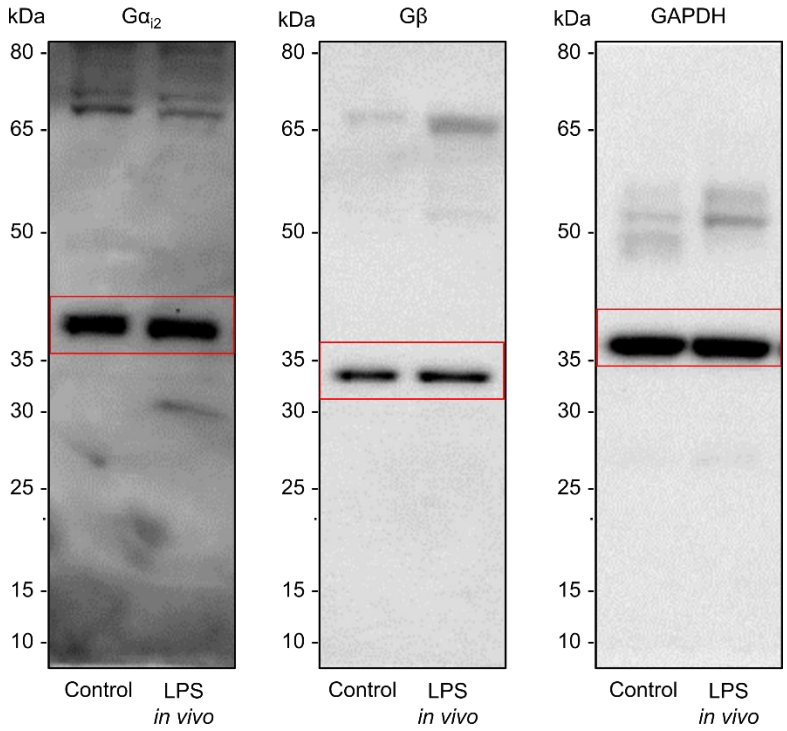

Fig. S6A

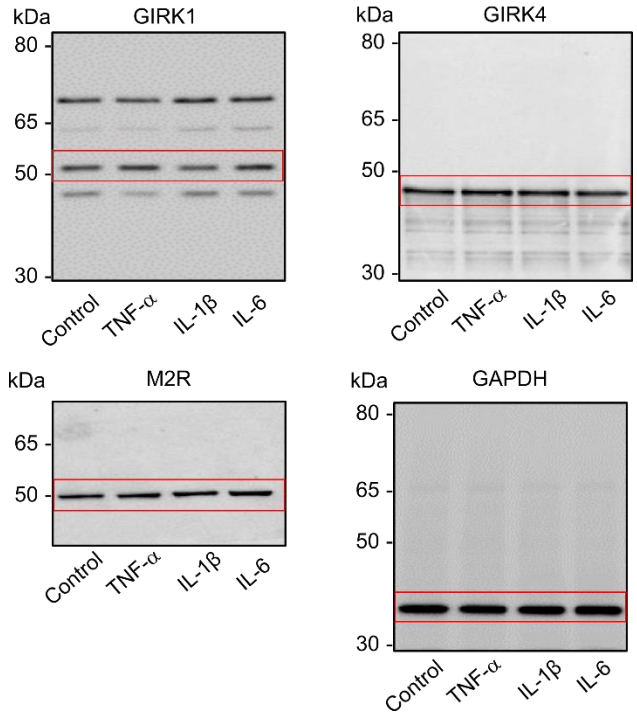

Fig. S7. Western blot images showing the specific protein band highlighted in each blot with reference to molecular weight. The highlighted bands correspond to the protein bands shown in the western blot images in Figs. 4A-B, S2A, S5A, S6A.